

Serial Polar Automorphism Ensemble Decoders for Physical Unclonable Functions

Marvin Rübenacke^{†,*}, Sebastian Cammerer[‡], Michael Sullivan[‡], and Alexander Keller[‡]

[†]University of Stuttgart, [‡]NVIDIA, contact: scammerer@nvidia.com

Abstract—Physical unclonable functions (PUFs) involve challenging practical applications of error-correcting codes (ECCs), requiring extremely low failure rates on the order of 10^{-6} and below despite raw input bit error rates as high as 22%. These requirements call for an efficient ultra-low rate code design. In this work, we propose a novel coding scheme tailored for PUFs based on Polar codes and a low-complexity version of automorphism ensemble decoding (AED). Notably, our serial AED scheme reuses a single successive cancellation (SC) decoder across multiple decoding attempts. By introducing cascaded and recursive interleavers, we efficiently scale the number of AED candidates without requiring expensive large multiplexers. An aggressive quantization strategy of only 3 bits per message further reduces the area requirements of the underlying SC decoder. The resulting coding scheme achieves the same block error rate of 10^{-6} as our baseline based on Bose–Ray–Chaudhuri–Hocquenghem (BCH) codes while requiring $1.75\times$ fewer codeword bits to encode the same $K = 312$ payload bits. This reduction translates directly into $1.75\times$ less helper data storage and, consequently, a smaller overall chip area.

I. INTRODUCTION

Physical Unclonable Functions (PUFs) generate a unique and unpredictable hardware fingerprint across semiconductor devices based on random variations of the manufacturing process that cannot be cloned [1]–[3]. Such perfectly secret information provides protection against copying, cloning, and readout by attackers—even when using intrusive or destructive techniques. One physical realization of a PUF involves reading bits from uninitialized static random-access memory (SRAM). While random across devices, an individual cell tends to output the same binary value when queried multiple times. Carefully combining the noisy PUF responses with a strong error-correcting code (ECC) scheme can guarantee reliable data extraction without leaking private information through helper data [2], [4]. As the reliability even depends on hardware parameters such as temperature and cell aging, heavily overdesigned ECC schemes are necessary.

Traditional approaches in academia mostly focus on concatenated codes that combine low-complexity repetition with modest-complexity Bose–Ray–Chaudhuri–Hocquenghem (BCH) codes [4], [5]. Such concatenated codes work well in moderate error-rate regimes but they do not scale gracefully to very high raw input error rates. As an alternative, Polar codes [6] have been proposed for PUFs [7], promising higher

code rates, though previous work mostly focused on successive cancellation (SC) decoding since the hardware complexity of successive cancellation list (SCL) decoding appears prohibitive for practical PUF applications.

In this work, we propose a serial variant of automorphism ensemble decoding (AED). AED was originally developed in the context of wireless communications [8]–[11], and it can achieve near-maximum likelihood (ML) decoding performance by applying multiple decoding attempts using permuted versions of the noisy codeword. However, scaling the number of AED candidates is potentially expensive, as it either requires many parallel SC decoders or large multiplexers for the interleavers/de-interleavers [12].

For efficient hardware re-use, the interleavers must be carefully optimized to avoid large multiplexers. In [13], the authors optimize the permutations to reduce implementation overhead, but do not consider their impact on decoding performance. We propose cascaded interleavers based on the fact that permutation automorphisms form a group, and thus a cascade of interleavers will produce another valid permutation of the original codeword. Additionally, even a single interleaver can recursively generate multiple permutations, which further reduces the area footprint while not compromising the decoding performance.

The main contributions of this work are a

- novel serial Polar AED reusing a single SC decoder,
- cascaded and recursive interleavers for AED that efficiently scale the number of candidates,
- binary input AED with aggressive 3-bit quantization, and
- very-large-scale integration (VLSI) synthesis results demonstrating area efficiency.

Throughout this work, vectors and matrices are denoted by boldface lowercase \mathbf{x} and uppercase \mathbf{A} letters, respectively. S_N denotes the symmetric group of degree N . For a permutation $\pi \in S_N$, $j = \pi(i)$ maps the indices $i \in \{0, 1, \dots, N-1\}$ to $j \in \{0, 1, \dots, N-1\}$, and we write $\mathbf{x}' = \pi(\mathbf{x})$ to denote the reordering of a vector $\mathbf{x} \in S_N$ according to $x'_{\pi(i)} = x_i$.

II. SYSTEM MODEL AND BACKGROUND

In the following, we introduce the serial version of AED in the context of PUFs which motivates the need for ultra-low rate codes and high area efficiency. Note that the proposed scheme can also be applied to any other communication or storage system. Fig. 1 shows an overview of the system.

*Work done during an internship at NVIDIA.

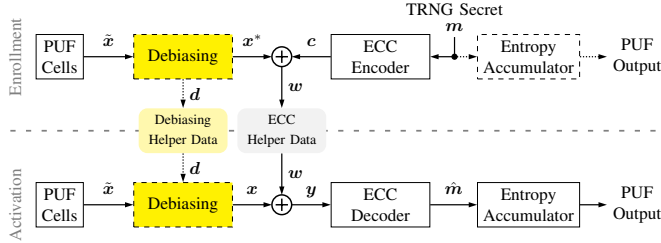


Fig. 1: Overview of the PUF key extraction pipeline using the fuzzy commitment scheme. The debiasing (yellow) is an optional component.

A. Physical Unclonable Functions

A PUF is modeled by $\mathbf{x} = \mathbf{x}^* \oplus \mathbf{e}$ and consists of N binary PUF cells $x_i \in \mathbb{F}_2$. The ground truth vector \mathbf{x}^* is called the *golden PUF response* that is only observable through a noisy channel. This channel is assumed to be a binary symmetric channel (BSC) with bit-flip probability ϵ and a noise vector \mathbf{e} with $e_i \sim \text{Ber}(\epsilon)$.

B. Helper Data Algorithms

To cope with the errors, an ECC is required. In general, a linear ECC is a K -dimensional subspace of the full N -dimensional space of possible PUF responses \mathbb{F}_2^N . For this reason, the probability that \mathbf{x}^* is a valid codeword (or close to a valid codeword) is vanishingly small. Therefore, the code space (or, equivalently, the PUF response) must be *offset* such that a codeword is close to the PUF response. This offset must be determined once and stored in non-volatile memory (fuses), in such a way that it does not leak any information about the secret. There exist several implementations of such an offset. We consider the commonly used *fuzzy commitment* code-offset helper data algorithm [4] as depicted in Fig. 1.

The operation of the PUF is split into two phases: *enrollment* and *activation*. At enrollment (e.g., in the factory), the golden PUF response \mathbf{x}^* is determined, for example by querying the PUF multiple times and performing majority voting. Moreover, a secret message $\mathbf{m} \in \mathbb{F}_2^K$ is either selected or randomly generated using a true random number generator (TRNG) and encoded into the codeword $\mathbf{c} = \mathbf{m}\mathbf{G}$. Then, the helper data $\mathbf{w} = \mathbf{c} \oplus \mathbf{x}^*$ is determined and stored in the fuses. At activation (i.e., at every device readout), the noisy PUF response \mathbf{x} is read out, and a vector close to the codeword $\mathbf{y} = \mathbf{x} \oplus \mathbf{w}$ is obtained. Since $\mathbf{y} = \mathbf{x} \oplus \mathbf{w} = \mathbf{x} \oplus \mathbf{x}^* \oplus \mathbf{c} = \mathbf{c} \oplus \mathbf{e}$, the codeword \mathbf{c} (or \mathbf{m}) can be recovered by applying the ECC decoder to \mathbf{y} to remove the error \mathbf{e} , assuming the error is within the error-correction capability of the code.

C. Polar Codes

An ($N = 2^n, K$) Polar code \mathcal{C} is constructed from the Polar transformation defined by the matrix $\mathbf{G}_N = [\begin{smallmatrix} 1 & 0 \\ 1 & 1 \end{smallmatrix}]^{\otimes n}$, where $(\cdot)^{\otimes n}$ denotes the n -fold application of the Kronecker product. This transformation, along with a successive decoding schedule, results in a polarization effect, i.e., some channels become virtually noiseless and can carry uncoded information.

The remaining channels are completely noisy. Hence they cannot carry information and are fixed to a known value (typically 0). The Polar code is defined by selecting these K reliable channels (or rows from the \mathbf{G}_N) called the information set \mathcal{I} , while the other $N-K$ row indices form the frozen set \mathcal{F} . The synthetic channels exhibit a partial order [14] with respect to their reliability. Thus, a Polar code is fully specified by a few generators \mathcal{I}_{\min} , and the remaining elements of \mathcal{I} are implied by the partial order [9]. Let $\mathbf{m} \in \mathbb{F}_2^K$ denote the payload (message) vector of K information bits. The fully uncoded vector $\mathbf{u} \in \mathbb{F}_2^N$ is constructed from the information bits \mathbf{m} in the information positions \mathcal{I} and zeros in the frozen positions \mathcal{F} . The codeword \mathbf{c} is obtained by computing $\mathbf{c} = \mathbf{u}\mathbf{G}_N$ using the arithmetic in \mathbb{F}_2 (i.e., modulo 2).

D. Successive Cancellation Decoding

Polar codes can be decoded using the SC algorithm [15]. For each bit u_i , SC decoding determines the most likely value based on the received vector \mathbf{y} and the previously decoded bits $\hat{u}_0 \dots \hat{u}_{i-1}$, where $\hat{u}_i = 0$ for frozen bits $i \in \mathcal{F}$. SC decoding can be formulated recursively on the factor tree in log-likelihood ratio (LLR) domain. Let ℓ denote the LLR vector corresponding to the \mathbf{y} . First, ℓ is split in two halves $\ell = (\ell_1 \mid \ell_2)$ and the output LLR for the first half is given as

$\ell'_{1,i} := f(\ell_{1,i}, \ell_{2,i}) := \text{sgn}(\ell_{1,i}) \text{sgn}(\ell_{2,i}) \min\{|\ell_{1,i}|, |\ell_{2,i}|\}$, which approximates $\tilde{f}(a, b) = \ln \frac{1+e^{a+b}}{e^a + e^b}$. Then, ℓ'_1 is decoded further recursively, resulting in the estimate \hat{c}'_1 . This is used to compute the output LLR for the second half as

$$\ell'_{2,i} := g(\ell_{1,i}, \ell_{2,i}, \hat{c}'_1) := (-1)^{\hat{c}'_1} \ell_{1,i} + \ell_{2,i},$$

and the decoding of ℓ'_2 is performed recursively, resulting in \hat{c}'_2 . The overall codeword estimate is then computed as $\hat{\mathbf{c}} = (\hat{c}'_1 \oplus \hat{c}'_2 \mid \hat{c}'_2)$. The recursion can be followed until the information bits u_i are reached. However, usually, larger leaf nodes are reached early, which are simple to decode, such as Rate-0, Repetition (Rep), single parity check (SPC), and Rate-1 codes [16]. In the following, let $\text{SC}(\mathbf{y})$ denote the decoding function that returns the codeword estimate $\hat{\mathbf{c}}$ using the SC decoding algorithm.

E. Permutation Automorphism Group

The (permutation) automorphism group of a code \mathcal{C} is the set of permutations $\pi \in S_N$ that map each codeword onto another (not necessarily different) codeword, i.e.,

$$\text{Aut}(\mathcal{C}) = \{\pi \mid \pi(\mathbf{c}) \in \mathcal{C} \ \forall \mathbf{c} \in \mathcal{C}\}.$$

The permutation automorphisms form a group under permutation composition, i.e., the following properties hold:

- $\text{id} \in \text{Aut}(\mathcal{C})$
- $\forall \pi, \sigma \in \text{Aut}(\mathcal{C}) : \pi \circ \sigma \in \text{Aut}(\mathcal{C})$, where $(\pi \circ \sigma)(i) = \pi(\sigma(i))$
- $\forall \pi \in \text{Aut}(\mathcal{C}) : \exists \pi^{-1} \in \text{Aut}(\mathcal{C})$ with $\pi \circ \pi^{-1} = \text{id}$.

The j -fold application of a permutation π (composition with itself) is denoted by π^j and the *order* $\text{ord}(\pi)$ is the smallest positive number j such that $\pi^j = \text{id}$.

Polar codes exhibit affine permutation automorphisms of the form

$$\mathbf{x}' = \mathbf{A}\mathbf{x} + \mathbf{b},$$

where \mathbf{x} and \mathbf{x}' are the least significant bit (LSB)-first binary representations¹ of the codeword indices i and $i' = \pi(i)$, respectively, $\mathbf{b} \in \mathbb{F}_2^n$ and $\mathbf{A} \in \mathbb{F}_2^{n \times n}$ is a block lower triangular invertible matrix with no non-zero elements above the block-diagonal given by a block profile \mathbf{s} . The block profile is uniquely defined by the information set \mathcal{I} of the Polar code [9]. This group is called the block lower-triangular affine (BLTA) group denoted by $\text{BLTA}(\mathbf{s})$. For $\mathbf{s} = [1, 1, \dots, 1]$, we have the lower-triangular affine (LTA) group denoted by $\text{LTA}(n)$.

F. Automorphism Ensemble Decoding

Automorphism ensemble decoding (AED) is a decoding algorithm that performs multiple decoding attempts on permuted versions of the noisy codeword \mathbf{y} [8]. To this end, a set of M permutations $\pi_j \in \text{Aut}(\mathcal{C})$ is selected and the output of the j -th SC decoding attempt is given by

$$\hat{\mathbf{c}}_j = \pi_j^{-1}(\text{SC}(\pi_j(\mathbf{y}))).$$

Out of these codeword candidates, the most likely codeword is selected as the final codeword estimate

$$\hat{\mathbf{c}} = \underset{0 \leq j < M}{\text{argmax}} p(\mathbf{y} \mid \hat{\mathbf{c}}_j).$$

In the following, SC-based AED with M permutations is denoted by $\text{AE-SC-}M$.

In [8], it was shown that for all $\pi \in \text{LTA}(n)$, $\pi_j^{-1}(\text{SC}(\pi_j(\mathbf{y}))) = \text{SC}(\mathbf{y})$, i.e., the permutation is *absorbed* by SC decoding and there is no gain in using these permutations in AED. Therefore, it is sufficient to consider linear permutations whose \mathbf{A} matrix is a product of a permutation matrix \mathbf{P} and an upper-triangular matrix \mathbf{U} bounded by the block profile \mathbf{s} [8], [17].

For ease of description, we consider the slightly more general set of invertible block-diagonal matrices \mathbf{A} with block sizes $\mathbf{s} = [s_0, s_1, \dots, s_{t-1}]$, called the block diagonal linear (BDL) group $\text{BDL}(\mathbf{s})$. Then $\mathbf{A} \in \text{BDL}(\mathbf{s})$ can be written as $\mathbf{A} = \text{diag}(\mathbf{A}_0, \mathbf{A}_1, \dots, \mathbf{A}_{t-1})$, where $\mathbf{A}_j \in \mathbb{F}_2^{s_j \times s_j}$ and invertible. As the sub-matrices \mathbf{A}_j do not interact and can be chosen independently, BDL is the direct group product

$$\text{BDL}(\mathbf{s}) = \text{GL}(s_0) \times \text{GL}(s_1) \times \dots \times \text{GL}(s_{t-1})$$

where $\text{GL}(m)$ denotes the general linear group of degree m over \mathbb{F}_2 . This leads to the following property about BDL permutations.

Theorem 1. *Let $\mathbf{P}(\mathbf{A})$ denote the $N \times N$ permutation matrix of codeword bits corresponding to the linear transformation matrix \mathbf{A} . For any block profile $\mathbf{s} = [s_0, s_1, \dots, s_{t-1}]$, and $\mathbf{A} = \text{diag}(\mathbf{A}_0, \mathbf{A}_1, \dots, \mathbf{A}_{t-1}) \in \text{BDL}(\mathbf{s})$, we have*

$$\mathbf{P}(\mathbf{A}) = \mathbf{P}(\mathbf{A}_0) \otimes \mathbf{P}(\mathbf{A}_1) \otimes \dots \otimes \mathbf{P}(\mathbf{A}_{t-1}).$$

¹As an exception, we are using column vectors here.

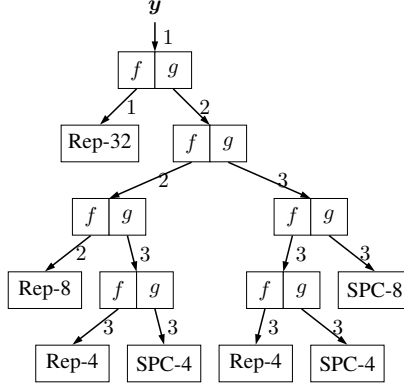


Fig. 2: Simplified SC decoding factor tree of a (64, 17) Polar code with LLR bit widths annotated; max. bit width is 3 bits.

Proof: The statement follows from the fact that BDL is a direct product of general linear groups [18, Ch. 3.2]. ■

Example 1. Let $\mathbf{s} = [2, 2]$, $\mathbf{A}_0 = \begin{bmatrix} 1 & 1 \\ 0 & 1 \end{bmatrix}$ and $\mathbf{A}_1 = \begin{bmatrix} 0 & 1 \\ 1 & 0 \end{bmatrix}$. \mathbf{A}_0 corresponds to the permutation $\pi_0 = [0, 1, 3, 2]$ and \mathbf{A}_1 to $\pi_1 = [0, 2, 1, 3]$. The overall permutation corresponding to $\mathbf{A} = \text{diag}(\mathbf{A}_0, \mathbf{A}_1)$ is $\pi = [0, 1, 3, 2, 8, 9, 11, 10, 4, 5, 7, 6, 12, 13, 15, 14]$, where there are four blocks of four elements each, which are permuted corresponding to π_0 and π_1 , respectively.

III. NON-UNIFORM QUANTIZATION

In contrast to wireless communications, where the decoder input \mathbf{y} is typically assumed to be the output of a Gaussian channel and of high resolution, the PUF scenario is equivalent to a BSC with bit-flip probability ϵ , i.e., $\mathbf{y} \in \mathbb{F}_2^N$. Assuming equally probable bits c_i , channel output LLR of the i -th bit can be computed as

$$\ell_i = \ln \frac{P(y_i | c_i = 0)}{P(y_i | c_i = 1)} = (-1)^{y_i} \ln \frac{1 - \epsilon}{\epsilon}.$$

Observe that SC decoding is invariant to constant scaling of the input LLRs. Therefore, the common factor $\ln \frac{1 - \epsilon}{\epsilon}$ can be dropped and only a single bit of precision is required for each input LLR $\ell_i \in \{\pm 1\}$ to the decoder.

As a consequence of the low input LLR resolution, the decoding can be non-uniformly quantized (meaning different bit widths for different variables) without any loss in performance. Let $\mathcal{V}(\ell)$ denote the set of different values that an LLR ℓ may take. A binary digital implementation of SC decoding requires $\lceil \log_2 |\mathcal{V}(\ell)| \rceil$ bits to represent the value ℓ . Observe that the f -function does not change the set \mathcal{V} , and hence does not increase the bit width to represent the outgoing LLRs. The g -function may output any of $\pm \ell_1 + \ell_2 \ \forall \ell_1 \in \mathcal{V}(\ell_1), \ell_2 \in \mathcal{V}(\ell_2)$, at most doubling the size of \mathcal{V} . Hence, at most one bit more is required for the output than the inputs of the g -function. To reduce implementation complexity, we propose to limit the number of different values to a power of two, namely the maximum bit width of the decoder. For an integer-based realization of the LLRs, we divide the value by 2 if all

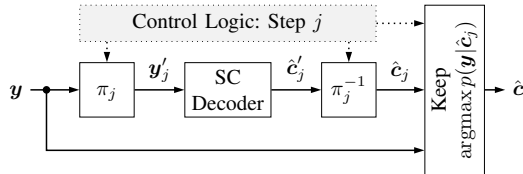


Fig. 3: Serial implementation of AED with a single constituent decoder and switchable permutations.

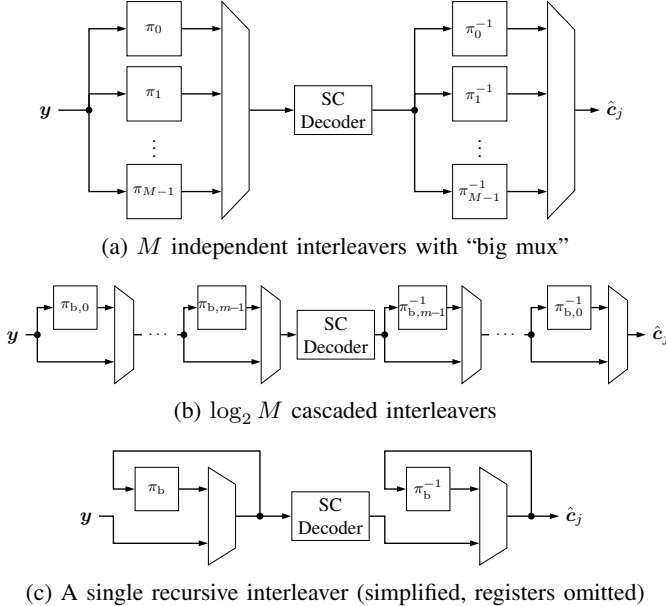


Fig. 4: Different interleaver architectures to realize the permutations in a serial AED implementation. The recursive de-interleaver requires multiple cycles which are not shown.

elements of \mathcal{V} are even. For example, after the first g -function with inputs ± 1 , the set of outputs is $\{-2, 0, +2\}$, which may be scaled down to $\{-1, 0, +1\}$, again due to the scaling invariance of SC decoding. Then, the values are clipped to q bits, saturating at $\pm(2^{q-1} - 1)$.

Fig. 2 shows the simplified factor tree of a (64, 17) Polar code with binary channel output and a maximum quantization bit width of 3 bits. A large portion of the tree only requires 1 or 2 bits of quantization. Furthermore, we observed that AE-SC decoding is more robust to low-resolution LLR quantizations when compared to pure SC decoding. Consequently, the proposed AE-SC decoder can operate with 3-bit message quantizations even for deeper factor trees. Fig. 6 shows an (1024, 78) Polar code with 3-bit message quantization compared to the 5-bit SC decoder. The corresponding 3-bit SC decoder is not shown, but its performance significantly degrades.

IV. SERIAL AUTOMORPHISM ENSEMBLE DECODING

A. Serial Architecture

Compared to other ensemble decoding schemes, the component decoders in AED are identical for each decoding attempt. Therefore, for applications without stringent latency

constraints, such as a PUF, it becomes viable to re-use the same decoder block for each decoding attempt in a sequential fashion and only multiplex in a different permutation, as shown in Fig. 3. Naïvely, the permutations can be implemented by M different, hard-wired interleavers, computing all y_j in parallel, and then selecting the one required for the current decoding attempt using a big multiplexer (“big mux”). This architecture is depicted in Fig. 4a. Given a binary input signal, each of the two big multiplexers needs to switch N parallel binary signals between M inputs. Note that, without loss of generality, one of the permutations may be the identity permutation.

B. Cascaded Interleavers

To reduce the complexity, we propose to select the permutations such that they are not completely independent anymore, but share common factors.

From m base permutations $\pi_{b,i}$, $M = 2^m$ permutations (including the identity permutation) are generated as

$$\pi_j = \prod_{i=0}^{m-1} \pi_{b,i}^{j_i},$$

where j_i denotes the i -th bit of the binary expansion of j . A possible realization of these permutations in the serial AED framework is depicted in Fig. 4b. The resulting circuit involves $\log_2(M)$ two-input multiplexers (for N parallel signals), which is in general much less complex than the single, M -input multiplexer. Moreover, only $\log_2(M)$ hard-wired interleavers are required, compared to the M interleavers in the independent case.

C. Recursive Interleavers

To even further reduce the implementation complexity, it is also possible to generate multiple permutations (including the identity permutation) from a single base permutation as its powers $\pi_j := \pi_b^j$. Formulated recursively, we have $\pi_j = \pi_b \circ \pi_{j-1}$, with $\pi_0 = \text{id}$. Therefore, the permutations π_j can be generated successively by routing the vector multiple times through an interleaver realizing π_b , as shown in Fig. 4c. Note that while the permutation stage before decoding can output a new permutation every clock cycle, the de-permutation stage has to run j times for the j -th permutation.

This approach can generate up to $M = \text{ord}(\pi_b)$ different permutations. For $\pi_b \in \text{BDL}(s)$ with transformation matrix $\mathbf{A} = \text{diag}(\mathbf{A}_0, \mathbf{A}_1, \dots, \mathbf{A}_{t-1})$, we have

$$\text{ord}(\pi_b) = \text{LCM}(\text{ord}(\mathbf{A}_0), \text{ord}(\mathbf{A}_1), \dots, \text{ord}(\mathbf{A}_{t-1})),$$

which is maximized for \mathbf{A}_i being Singer cycles with $\text{ord}(\mathbf{A}_i) = 2^{s_i} - 1$ [19].

D. Block Interleavers

Independent of the realization of the permutations (e.g., cascaded or recursive), the size of the interleavers may be reduced by applying the same interleaver pattern multiple times to neighboring symbols (i.e., in a block-wise fashion). While BDL eliminates already many SC-equivariant permutations from BLTA, more permutations are absorbed by SC decoding.

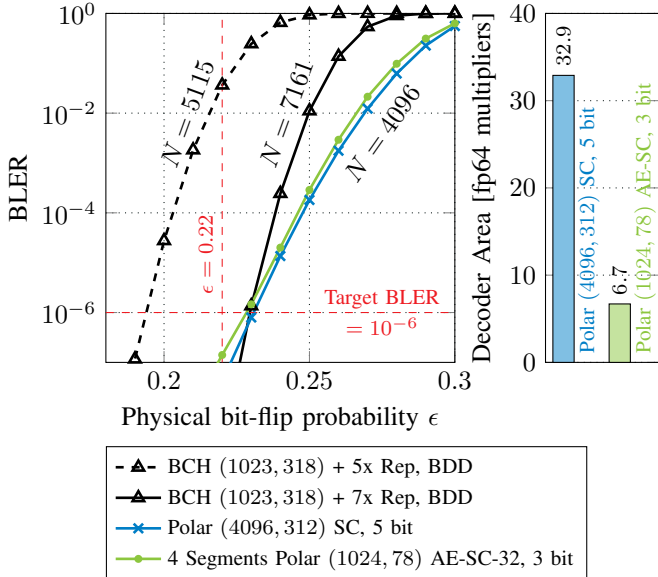


Fig. 5: Comparison of BCH and Polar-based coding schemes for $K \approx 312$.

In particular, the block of size s_0 in the upper left corner of \mathbf{A} is absorbed if all size 2^{s_0} constituent codes are either rate-0, rate-1, repetition or SPC codes, for which the SC algorithm is ML, and thus equivariant [20], [21]. In these cases, one can set $\mathbf{A}_0 = \mathbf{I}_{s_0}$ without any loss in performance.

Even when they are non-equivariant, the AED gain is smaller for small blocks in the top left of \mathbf{A} [9]. Therefore, to save implementation complexity, it may be beneficial to also set $\mathbf{A}_0 = \mathbf{I}_{s_0}$ in these cases. The permutations move blocks of $b = 2^{s_0}$ neighboring symbols based on a permutation $\sigma \in \text{BDL}([s_1, \dots, s_{t-1}])$, i.e.,

$$\begin{aligned} \pi = & [\sigma(0), \sigma(0) + 1, \dots, \sigma(0) + b - 1, \\ & \sigma(1), \sigma(1) + 1, \dots, \sigma(1) + b - 1, \dots, \\ & \sigma(N/b - 1), \sigma(N/b - 1) + 1, \dots, \sigma(N/b - 1) + b - 1]. \end{aligned}$$

Example 2. Let $s = [2, 2]$, with $\mathbf{A}_1 = \begin{bmatrix} 0 & 1 \\ 1 & 0 \end{bmatrix}$. We set $\mathbf{A}_0 = \mathbf{I}_2$. The overall permutation is $\pi = [0, 1, 2, 3, 8, 9, 10, 11, 4, 5, 6, 7, 12, 13, 14, 15]$, where blocks of size $b = 4$ stay together.

Therefore, again at the cost of increased latency, the permutation π can be realized by applying the small permutation σ b times in a bit-serial fashion.

V. RESULTS

A. Comparison of ECC Architectures

We target a PUF scenario with payload size of $K = 312$ bits that should attain a maximum activation failure rate (block error rate (BLER)) of 10^{-6} at worst-case physical bit-flip probability $\epsilon = 0.22$.

Fig. 5 compares the proposed Polar-AED scheme with other ECC architectures. The best possible baseline system with BCH and bounded distance decoding (BDD) codes consists

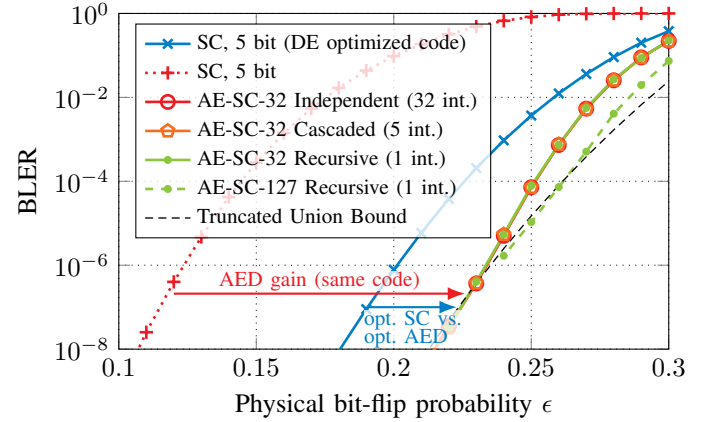


Fig. 6: Error-rate performance results for different interleaver realizations for the (1024, 78) code with $\mathcal{I}_{\min} = [255, 505]$.

of an (1023, 318), 91-error-correcting BCH code and an inner 7-fold repetition code. Note that 5-fold repetition is not enough to meet the constraints. Secondly, we consider a single (4096, 312) Polar code designed using density evolution (DE) [22] for 5-bit SC decoding. By utilizing the more powerful AED decoder with $M = 32$ permutations, we can achieve the same performance using four segments of a (1024, 78) Polar code and only 3-bit SC, resulting in a decoder footprint that is five times smaller. Areas are normalized to a pipelined double-precision floating-point multiplier, which serves as a proxy for a sizeable logic component. Note that all segments must be correctly decoded, so the BLER approximately quadruples compared to the single segment case. The (1024, 78) code was found using the symmetric partial order [23] for the fixed block profile $s = [3, 7]$ and has minimum information set $\mathcal{I}_{\min} = \{255, 505\}$. All its $2^{s_0} = 8$ bit SC leaf node decoders are ML decoders, and hence, bit permutations within the three least significant bits are equivariant.

The performance of all systems is roughly equal at the target operating point. However, the BCH+Repetition system requires codewords that are 1.75 times as long (and, thus, 75 % more PUF cells and fuses) as the Polar code based schemes.

B. Permutation Selection and Realization

Although a random selection of the permutations in AED works well in practice, it can sometimes result in poorly performing ensembles. Therefore, for each interleaver realization, we optimize the selection of the permutations using the greedy, data-driven approach proposed in [11].

Fig. 6 compares different decoding approaches for the (1024, 78) code with $\mathcal{I}_{\min} = [255, 505]$. We consider SC decoding with 5-bit quantization, which is approximately equal to full-precision decoding, and AED with 3-bit quantization. For the symmetric code design, AED with $M = 32$ achieves a BLER of 10^{-6} at double the physical error rate, even with its coarser quantization. Furthermore, the interleaver realizations show virtually identical performance, indicating no loss from the proposed cascaded or recursive interleaver designs. Finally,

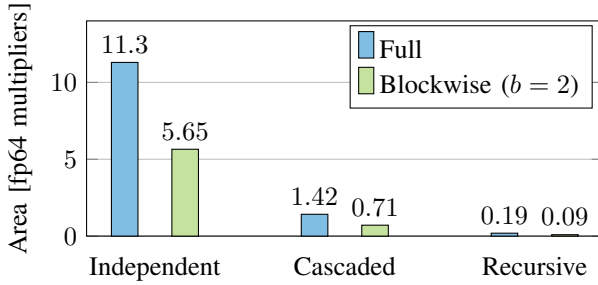


Fig. 7: Normalized hardware area of different interleaver realizations for $N = 1024$ AE-SC-128. Area is normalized to a double-precision floating-point multiplier.

as a baseline we show the best possible (1024, 78) Polar code for 5-bit SC decoding obtained from DE. While this code performs better under SC decoding, the symmetric code outperforms it with AED. The recursive interleaver uses a Singer cycle in the non-equivariant part, yielding up to $2^7 - 1 = 127$ decoding paths; it is the best-performing curve, and it closely follows the truncated union bound of the code.

C. Interleaver Implementation Complexity

We compare the hardware overheads of different interleavers using Verilog designs synthesized by the Synopsys toolchain with a modern 3 nm industrial technology library. Fig. 7 compares the post-synthesis area of a permutation unit of a $N = 1024$ AE-SC-128 decoder using independent permutations (i.e., “big mux”) to our optimized cascaded and recursive designs. Both a full and blockwise interleaver ($b = 2$) are shown. The independent interleavers consume significant logic area, requiring the equivalent of $> 10 \times$ (non-blockwise) or $> 5 \times$ (blockwise) multipliers. The cascaded interleavers reduce the area to a more practical < 1.5 multiplier-equivalents, while the recursive interleaver operates using only a single level of two-input multiplexing, reducing its area to a nominal size. The area of a multiplexer is roughly quadratic with its number of inputs, meaning that larger interleavers with more than 128 permutations would scale quadratically, while those with larger codeword sizes should scale linearly. At large codeword sizes or a large number of permutations, cascaded or recursive interleaving become imperative to avoid an explosion of complexity.

VI. EXTENSION TO BIASED PUFs

Ideally, PUF cells are unbiased, meaning $x_i \sim \text{Ber}(p)$ with $p = 0.5$ across devices. However, if $p \neq 0.5$, the asymmetric tendency towards 0 or 1 will indicate a global bias and the entropy of \mathbf{x} will be reduced and helper data \mathbf{w} may leak information about \mathbf{x}^* [5]. In such cases, debiasing is a remedy to maintain system security. As depicted in Fig. 1, debiasing is applied at the output of the PUF cells. An efficient debiasing scheme is von Neumann with pair output (VNPO) [5], which considers PUF cell pairs. At enrollment, pairs with identical values are discarded and kept pair positions are

stored in debiasing helper data \mathbf{d} . If one of the bits of the kept pairs is flipped, an implicit two-fold repetition code will be formed. Moreover, larger inner repetition codes may be beneficial to obtain low-rate codes with small decoder footprints. When the corresponding values are combined, higher-precision LLRs will be formed that can be naturally processed by Polar decoders. Our proposed AED scheme can therefore be straightforwardly applied to PUFs with debiasing when the input bit width is increased accordingly. Note that the concept of block interleavers can also be applied here, either for the bits of the independent observations which are combined after interleaving, or the quantized LLR representations if combined before interleaving.

VII. CONCLUSION

In this work, we proposed a novel serial AED scheme for Polar codes combining competitive error rate performance with high area efficiency. Our approach introduces cascaded and recursive interleavers that efficiently scale the number of AED candidates without requiring expensive large multiplexers, enabling practical hardware implementation. The proposed aggressive 3-bit quantization strategy significantly reduces decoder complexity while maintaining near-ML decoding performance, demonstrating the robustness of AED to quantization effects. Our coding scheme achieves the same 10^{-6} block error rate as BCH-based baselines while requiring $1.75 \times$ fewer codeword bits, directly translating to reduced helper data storage and chip area. Contrary to classical BCH decoders, the proposed scheme naturally supports soft-decoding, opening a plethora of potential use cases.

REFERENCES

- [1] G. E. Suh and S. Devadas, “Physical Unclonable Functions for Device Authentication and Secret Key Generation,” in *Proceedings of the 44th Annual Design Automation Conference*, 2007, pp. 9–14.
- [2] O. Günlü, O. İşcan, V. Sidorenko, and G. Kramer, “Code Constructions for Physical Unclonable Functions and Biometric Secrecy Systems,” *IEEE Transactions on Information Forensics and Security*, vol. 14, no. 11, pp. 2848–2858, 2019.
- [3] M. Bloch, O. Günlü, A. Yener, F. Oggier, H. V. Poor, L. Sankar, and R. F. Schaefer, “An Overview of Information-Theoretic Security and Privacy: Metrics, Limits and Applications,” *IEEE Journal on Selected Areas in Information Theory*, vol. 2, no. 1, pp. 5–22, 2021.
- [4] J. Delvaux, D. Gu, D. Schellekens, and I. Verbauwhede, “Helper Data Algorithms for PUF-Based Key Generation: Overview and Analysis,” *IEEE Transactions on Computer-Aided Design of Integrated Circuits and Systems*, vol. 34, no. 6, pp. 889–902, 2015.
- [5] R. Maes, V. van der Leest, E. van der Sluis, and F. M. J. Willems, “Secure Key Generation from Biased PUFs: Extended Version,” *Journal of Cryptographic Engineering*, vol. 6, no. 2, pp. 121–137, 2016. [Online]. Available: <https://doi.org/10.1007/s13389-016-0125-6>
- [6] E. Arıkan, “Channel Polarization: A Method for Constructing Capacity-Achieving Codes for Symmetric Binary-Input Memoryless Channels,” *IEEE Trans. on Inf. Theory*, vol. 55, no. 7, pp. 3051–3073, 2009.
- [7] B. Chen, T. Ignatenko, F. M. J. Willems, R. Maes, E. van der Sluis, and G. Selimis, “A Robust SRAM-PUF Key Generation Scheme Based on Polar Codes,” in *2017 IEEE Global Comm. Conf. (GLOBECOM)*, 2017.
- [8] M. Geiselhart, A. Elkelesh, M. Ebada, S. Cammerer, and S. ten Brink, “Automorphism Ensemble Decoding of Reed–Muller Codes,” *IEEE Transactions on Communications*, vol. 69, no. 10, pp. 6424–6438, 2021.
- [9] ———, “On the Automorphism Group of Polar Codes,” in *2021 IEEE Int. Symp. on Information Theory (ISIT)*, 2021, pp. 1230–1235.
- [10] C. Pillet, V. Bioglio, and I. Land, “Polar Codes for Automorphism Ensemble Decoding,” in *IEEE Inf. Theory Workshop (ITW)*, 2021.

- [11] C. Kestel, M. Geiselhart, L. Johannsen, S. ten Brink, and N. Wehn, “Automorphism Ensemble Polar Code Decoders for 6G URLLC,” in *Int. ITG Workshop on Smart Antennas (WSA) and Conf. on Systems, Commun., and Coding (SCC)*, Braunschweig, Germany, Mar. 2023.
- [12] Y. Ren, Y. Shen, L. Zhang, A. T. Kristensen, A. Balatsoukas-Stimming, E. Boutilhon, A. Burg, and C. Zhang, “High-Throughput and Flexible Belief Propagation List Decoder for Polar Codes,” *IEEE Transactions on Signal Processing*, vol. 72, pp. 1158–1174, 2024.
- [13] J. Li, H. Zhou, R. Seah, and W. Gross, “Automorphism Ensemble Decoding of Polar Codes with Reduced Number of Routes,” in *2025 13th Int. Symp. on Topics in Coding (ISTC)*. IEEE, Aug 2025, pp. 1–5.
- [14] M. Bardet, V. Dragoi, A. Otmani, and J. Tillich, “Algebraic Properties of Polar Codes From a New Polynomial Formalism,” in *IEEE Inter. Symp. Inf. Theory (ISIT)*, 2016, pp. 230–234.
- [15] G. Schnabl and M. Bossert, “Soft-decision Decoding of Reed–Muller Codes as Generalized Multiple Concatenated Codes,” *IEEE Transactions on Information Theory*, vol. 41, no. 1, pp. 304–308, 1995.
- [16] A. Alamdar-Yazdi and F. R. Kschischang, “A Simplified Successive-Cancellation Decoder for Polar Codes,” *IEEE Communications Letters*, vol. 15, no. 12, pp. 1378–1380, 2011.
- [17] V. Bioglio, I. Land, and C. Pillet, “Group Properties of Polar Codes for Automorphism Ensemble Decoding,” *IEEE Transactions on Information Theory*, vol. 69, no. 6, pp. 3731–3747, 2023.
- [18] J.-P. Serre, *Linear Representations of Finite Groups*. New York: Springer-Verlag, 1977, translated from the second French edition by Leonard L. Scott, Graduate Texts in Mathematics, Vol. 42.
- [19] M. D. Hestenes, “Singer Groups,” *Canadian Journal of Mathematics*, vol. 22, no. 3, pp. 492–513, 1970.
- [20] C. Pillet, V. Bioglio, and I. Land, “Classification of Automorphisms for the Decoding of Polar Codes,” in *ICC 2022 - IEEE International Conference on Communications*, 2022, pp. 110–115.
- [21] Z. Ye, Y. Li, H. Zhang, R. Li, J. Wang, G. Yan, and Z. Ma, “The Complete SC-Invariant Affine Automorphisms of Polar Codes,” in *2022 IEEE Int. Symp. on Information Theory (ISIT)*, 2022, pp. 2368–2373.
- [22] R. Mori and T. Tanaka, “Performance and Construction of Polar Codes on Symmetric Binary-Input Memoryless Channels,” in *2009 IEEE International Symposium on Information Theory*, 2009, pp. 1496–1500.
- [23] M. Geiselhart, J. Clausius, and S. ten Brink, “Rate-Compatible Polar Codes for Automorphism Ensemble Decoding,” in *2023 12th International Symposium on Topics in Coding (ISTC)*, 2023, pp. 1–5.